



DOI: 10.29026/oea.2019.190006

# Lanthanide-based downshifting layers tested in a solar car race

Sandra F. H. Correia<sup>1</sup>, Ana R. N. Bastos<sup>1</sup>, Lianshe Fu<sup>1</sup>, Luís D. Carlos<sup>1</sup>, Paulo S. André<sup>2,3\*</sup> and Rute A. S. Ferreira<sup>1\*</sup>

The mismatch between the AM1.5G spectrum and the photovoltaic (PV) cells absorption is one of the most limiting factors for PV performance. To overcome this constraint through the enhancement of solar energy harvesting, luminescent downshifting (LDS) layers are very promising to shape the incident sunlight and, thus, we report here the use of Tb<sup>3+</sup>- and Eu<sup>3+</sup>-doped organic-inorganic hybrid materials as LDS layers on Si PV cells. Electrical measurements on the PV cell, done before and after the deposition of the LDS layers, confirm the positive effect of the coatings on the cell's performance in the UV spectral region. The maximum delivered power and the maximum absolute external quantum efficiency increased 14% and 27%, respectively. Moreover, a solar powered car race was organized in which the small vehicle containing the coated PV cells presented a relative increase of 9% in the velocity, when compared to that with the uncoated one.

**Keywords:** photovoltaics; downshifting layers; solar car; organic-inorganic hybrids; lanthanide ions

Correia S F H, Bastos A R N, Fu L S, Carlos L D, André P S *et al.* Lanthanide-based downshifting layers tested in a solar car race. *Opto-Electron Adv* 2, 190006 (2019).

## Introduction

The mismatch between the AM1.5G spectrum and the photovoltaic (PV) cells absorption is one of the most important factors contributing to limit the maximum efficiency of the cells, accounting for the losses associated with the excess energy of the absorbed above-bandgap energy photons and with the non-absorption of photons with energy below the bandgap of the PV cell. Also, in diffuse radiation conditions, the performance of crystalline silicon (c-Si) PV cells is greatly impaired, because clouds (water-vapour) absorbs mostly in the visible and near infrared (NIR) spectral regions, overlapping the c-Si PV cells highest performance spectral range (cell sensitivity decreases with increasing air mass). Thus, under cloudy skies the available radiation on Earth has a larger contribution (30%) of the shorter wavelengths (those not absorbed by water), when compared with that found in sunny days<sup>1,2</sup>. So, in locations where the most part of

solar irradiance is diffuse (cloudy skies), mirrors and concentration systems are mandatory to maximise c-Si PV cells performance<sup>3</sup>.

One way to overcome these losses is by shaping the incident sunlight through the use of luminescent downshifting (LDS) layers<sup>4,5</sup>, a relatively direct and cost-effective method to improve conversion efficiency of PV cells. These converting layers are coatings directly applied on the PV cell surface that are able to absorb the incident radiation unused by the PV cell which is then re-emitted at a usable wavelength (or refracted towards the PV cell)<sup>6,7</sup>. Moreover, these LDS layers reveal analogous optical efficiency under diffuse or direct radiation, thus, providing analogous output under cloudy days, which does not happen for bare PV cells. Another factor which could affect the efficiency of PV cells is their surface reflection of incident solar radiation. Regarding this issue, these LDS layers may also act as an antireflective coating and increase the amount of absorbed photons<sup>8</sup>.

<sup>1</sup>Department of Physics and CICECO - Aveiro Institute of Materials, University of Aveiro, 3810-193 Aveiro, Portugal; <sup>2</sup>Department of Electric and Computer Engineering and Instituto de Telecomunicações, Instituto Superior Técnico, Universidade de Lisboa, 1049-001 Lisbon, Portugal; <sup>3</sup>Department of Electronics, Telecommunications and Informatics, Instituto de Telecomunicações, University of Aveiro, Campus Universitário de Santiago, 3810-193 Aveiro, Portugal.

\*Correspondence: P S André, E-mail: paulo.andre@av.it.pt; R A S Ferreira, E-mail: rferreira@ua.pt

Received: 5 March 2019; Accepted: 24 April 2019; Published: 19 June 2019

Several studies showing improvements in solar cells performance with distinct LDS phosphors were reported, such as organic dyes<sup>9,10</sup>, quantum dots (QDs)<sup>9</sup>, and lanthanide ions ( $\text{Ln}^{3+}$ ) coordination complexes<sup>6,7,9–18</sup>. The reasons for the wide utilization of  $\text{Ln}^{3+}$  complexes (europium,  $\text{Eu}^{3+}$ , and terbium,  $\text{Tb}^{3+}$ ) are related to their strong emission and photostability and also the emission profile in the visible spectral range, which overlaps the absorption of c-Si solar cells. Moreover,  $\text{Eu}^{3+}$  and  $\text{Tb}^{3+}$  based materials display significantly larger ligands-induced Stokes shifts, when compared to organic dyes or QDs, minimizing the losses by self-absorption<sup>19</sup>.

In this work, we report  $\text{Eu}^{3+}$ - and  $\text{Tb}^{3+}$ -doped organic-inorganic hybrids (e.g., the d-U(600) di-ureasil and the t-U(5000) tri-ureasil) to be used as LDS coatings on Si-based PV cells. The materials were chosen based on the fact that they have similar absorption range (in the UV spectral region) and large absolute emission quantum yield ( $\Phi$ ) values ( $>0.50$ ), but present emission in distinct spectral regions. Two distinct strategies were adopted: (i) using the doped organic-inorganic hybrids coating as a substitute of the polymeric layer typically found on top of PV panels and (ii) depositing these materials as a coating directly on the top of PV cells in which the surface is sealed with polyethylene terephthalate polymer. The PV cells of approach (ii) were then attached to a small solar vehicle and its velocity was compared to one with a bare PV cell, in a horizontal plane.

## Experimental section

### Materials and methods

The diamine  $\alpha$ ,  $\omega$ -diaminepoly (oxyethylene-co-oxypropylene) (ED-600, commercially named Jeffamine<sup>®</sup> ED-600, Huntsman), 3-isocyanatepropyltriethoxysilane (ICPTES, 95%, Aldrich), salicylic acid (SA), sodium hydroxide (NaOH), tetrahydrofuran (THF, 99%, Sigma-Aldrich), absolute ethanol (EtOH, Sigma-Aldrich), europium chloride ( $\text{EuCl}_3 \cdot 6\text{H}_2\text{O}$ , 99%, Sigma-Aldrich), 2-thenoyltrifluoroacetone (Htta, Sigma-Aldrich) and hexane ( $\geq 95\%$ , Sigma-Aldrich) are all commercially available.  $\text{TbCl}_3$  aqueous solution (0.1 mol/L) was obtained by dissolving terbium oxide ( $\text{Tb}_4\text{O}_7$ ) in hydrochloride acid (HCl), the remaining acid was removed by evaporation, and the resulting solid was dissolved in distilled water. All chemicals were used as received without purifications.

### Synthesis of the d-U(600) doped with SA sensitized $\text{TbCl}_3$

For the case of  $\text{Tb}^{3+}$ -based organic-inorganic hybrids, a salicylic acid complex was used, since the use of SA as luminescence sensitizer for  $\text{Ln}^{3+}$  ions was proved effective as reported in some studies, mainly for analytical chemistry<sup>20,21</sup>, and these complexes were also suggested for PV applications in luminescent solar concentrators (LSCs) when incorporated in a polymer host<sup>22</sup>. The use of  $\text{Tb}^{3+}$ -based complexes involving the SA ligand in silica-

based sol-gel derived host materials has been tested with proved enhancement in the fluorescence intensity of  $\text{Tb}^{3+}$  ions when these chelates were doped in silica gel glasses due to a decrease in non-radiative transitions<sup>23,24</sup>. The precursor d-UPTES(600) was prepared according to the literature<sup>25</sup>. An amount of 1.371 mL (0.1371 mmol) of  $\text{TbCl}_3$  was added to a beaker and dried at 95 °C to evaporate the water. Then 0.5 g (0.4566 mmol) of d-UPTES(600) was added, followed by addition of 5 mL (or 10 mL) of EtOH. The mixture was stirred at room temperature to get a clear solution. Then 50  $\mu\text{L}$  of 0.05 mol/L HCl was added and stirred at room temperature for 30 minutes. 56.7 mg (0.4105 mmol) of SA was added, stirred for some time, and finally 0.41 mL of 1.0 mol/L NaOH was added. The molar ratio of d-UPTES(600): $\text{TbCl}_3$ :SA:NaOH=1:0.3:0.9:0.9. The d-U(600) organic-inorganic hybrid material doped with SA sensitized  $\text{TbCl}_3$  will be hereafter designated as dU6-Tb.

### Synthesis of the tripodal tri-ureasil, t-U(5000), organic-inorganic hybrid doped with $\text{Eu}(\text{tta})_3 \cdot 2\text{H}_2\text{O}$

The  $\text{Eu}(\text{tta})_3 \cdot 2\text{H}_2\text{O}$  complex was chosen because of its high  $^5\text{D}_0$  quantum efficiency ( $q = 0.74$ )<sup>26</sup>, that must correspond to one of the highest  $\Phi$  values of hybrid materials as  $q$  is the theoretical maximum value for  $\Phi$ . Moreover, after incorporation into the hybrid host, the water molecules coordinated to the  $\text{Eu}^{3+}$  ions will be replaced by the oxygen atoms from the carbonyl groups of the urea cross linkages contributing to suppress the  $\text{Eu}^{3+}$  emission quenching. In addition, this complex incorporated into hybrid matrices was already used for photovoltaic applications as optically active layers in LSCs<sup>27–29</sup>. The precursor t-UPTES(5000) was prepared according to the literature<sup>30</sup> and the synthesis of the  $\text{Eu}(\text{tta})_3 \cdot 2\text{H}_2\text{O}$  complex is fully described elsewhere (ESI for details)<sup>26,29</sup>. The  $\text{Eu}(\text{tta})_3 \cdot 2\text{H}_2\text{O}$  complex was incorporated into the non-hydrolysed precursor, by using 30 mg of  $\text{Eu}(\text{tta})_3 \cdot 2\text{H}_2\text{O}$  complex dissolved in 1.12 mL of EtOH and added to 1.5 g of t-UPTES(5000) in the presence of  $2.0 \times 10^{-2}$  mL HCl (1 M). The t-U(5000) organic-inorganic hybrid material doped with the  $\text{Eu}(\text{tta})_3 \cdot 2\text{H}_2\text{O}$  complex will be hereafter designated as tU5-Eu.

### LDS coatings fabrication

The dU6-Tb and tU5-Eu materials were deposited on the c-Si PV panels composed by 8 PV cells connected in series (KXOB22-01X8F, IXYS, after removal of the ethylene-vinyl acetate coating), designated hereafter as PV-1, and on c-Si PV cells which were posteriorly attached to a wheeled structure which composes small solar vehicles (Solar Racer, Geo Kids), designated hereafter as PV-2, by spin-coating at 500 rpm, for 30 s, using a volume of 0.1 mL (PV-1) and 0.2 mL (PV-2). Then, the devices were kept in the oven at 45 °C for 48 h together with bare PV cells. The performance of the bare PV devices is not affected by this mild heat treatment (Fig. S1 in ESI). The synthesized luminescent materials were also deposited in

glass substrates using the same conditions for structural and optical characterization.

#### UV/visible absorption and reflectance

UV/visible absorption and reflectance spectra were measured using a Lambda 950 dual-beam spectrometer (Perkin-Elmer).

#### Optical microscopy

Optical microscopy was used to measure the coatings thickness using an Olympus BX51 brightfield microscope (10× objective), in the reflection mode, equipped with a hyperspectral imaging system (CytoViva Inc., Auburn, AL). The system integrates an optical imaging CCD camera (QImaging Retiga 4000R), a visible-near-infrared hyperspectral camera (Cytoviva®), a motorized stage and a halogen light source (Fiber-lite®, DC-950). For the dU6-Tb and tU5-Eu, thickness values of  $5.7 \pm 0.5 \mu\text{m}$  and  $45 \pm 3 \mu\text{m}$  were measured, respectively (Fig. S2 in ESI). The differences in the thickness are due to the amount of solvent of the synthesis procedure for each sol, which determines their initial viscosity.

#### Photoluminescence spectroscopy

The photoluminescence spectra were recorded at room temperature with a modular double-grating excitation spectrofluorimeter with a TRIAX 320 emission monochromator (Fluorolog-3, Horiba Scientific) coupled to an R928 Hamamatsu photomultiplier.

#### Absolute emission quantum yield

The absolute emission quantum yield values were measured at room temperature using a system (Quantaaurus-QY Plus C13534, Hamamatsu) with a 150 W xenon lamp coupled to a monochromator for wavelength discrimination, an integrating sphere as the sample chamber, and a multichannel analyzer for signal detection. The method is accurate to within 10%.

#### Spectroscopic ellipsometry

The spectroscopic ellipsometry measurements were performed on the LDS coatings deposited on glass substrates using an AutoSE ellipsometer (HORIBA Scientific) with a total of 250 points in the wavelength interval 450–850 nm, an incidence angle of  $70^\circ$  and a signal quality of 30. A measurement spot area of  $250 \mu\text{m} \times 250 \mu\text{m}$  was used. Three measurements were performed in each sample. Due to differences in the thickness values, for the tU5-Eu coatings, the refractive index dispersion curves (Fig. S3 in ESI) were determined by direct inversion of the ellipsometric parameters; for the case of the dU6-Tb coating, a structural model consisting of a double-layered structure incorporating the LDS layer and air as ambient medium with a refractive index value of 1.00 was used. The dispersion curve was, then, determined using Cauchy absorbent model, given by:

$$n(\lambda) = A + \frac{B}{\lambda^2} + \frac{C}{\lambda^4}, \quad (1)$$

where  $n(\lambda)$  is the refractive index,  $\lambda$  is the wavelength and  $A = 1.5 \pm 0.1$ ,  $B = (6.0 \pm 0.1) \times 10^3 \text{ nm}^2$  and  $C = 2.0 \pm 0.6 \text{ nm}^4$ .

#### External quantum efficiency (EQE) and voltage-power (V-P) curves

The EQE was calculated as follows:

$$EQE(\lambda) = \frac{I_{sc} \cdot h \cdot c}{P_{in} \cdot e \cdot \lambda}, \quad (2)$$

where  $e$  is the charge of the electron,  $h$  is the Planck constant, and  $c$  is the speed of light. The solar simulator was coupled to a monochromator (Triax 180, Horiba Scientific). The short-circuit current ( $I_{sc}$ ) and the incident power ( $P_{in}$ ) values were measured using a sourcemeter device (2400 SourceMeter SMU Instruments, Keithley) and a c-Si calibrated photodiode (FDS1010, Thorlabs), respectively. The V-P curves were determined under AM1.5G simulated radiation (model 10500, Abet Technologies) using a semiconductor device analyzer (B1500A, Keysight Technologies). The tolerance of the measured EQE and V-I curves of the PV devices (as received from the manufacturer) is 5%.

#### Solar car race

The PV-2 cells ( $2.4 \text{ cm} \times 2.7 \text{ cm}$ ) were coupled to a wheeled structure composing a small scale prototype solar-powered car, with dimension of  $2.1 \text{ cm} \times 3.0 \text{ cm}$  and an  $1.1 \times 10^{-2} \text{ W}$  electrical motor. The electrical output power measured for all the PV-2 cells is the same. The solar race was performed on a plastic track with 1.2 m length and  $2 \times 10^{-2} \text{ m}$  width. The photo finish images were acquired with a smartphone camera with resolution of  $1920 \text{ pixel} \times 1080 \text{ pixel}$  (424 ppi), aperture of  $f/2.0$  and a sensor dimension of  $1/3.0''$  with  $1.12 \mu\text{m}$  pixel size. The time measurements were performed with a digital chronometer (NOVEDUC) with an infrared photocell, in 2 cm track pieces.

## Results and discussion

#### Optical characterization

The LDS coatings produced in the scope of this work were deposited in the PV-1 and in PV-2 devices, revealing the materials' emission under UV irradiation, Fig. 1 and Fig. S4 in ESI.

In particular, Fig. 2(a) shows the room-temperature emission spectra of the LDS coatings excited at the wavelength that maximizes the emission intensity. The emission spectra of dU6-Tb and tU5-Eu display the  $^3\text{D}_4 \rightarrow ^7\text{F}_{6-3}$  ( $\text{Tb}^{3+}$ ) and  $^5\text{D}_0 \rightarrow ^7\text{F}_{0-4}$  ( $\text{Eu}^{3+}$ ) transitions, respectively. In both cases, the absence of ligands and hybrids intrinsic emission indicates effective energy transfer to the  $\text{Ln}^{3+}$  ions, as demonstrated in the excitation spectra.

The excitation spectra were monitored at the transitions above mentioned, Fig. 2(a). For dU6-Tb, the spectra present three main components ascribed to the SA organic ligand ( $\sim 240 \text{ nm}$  and  $\sim 290 \text{ nm}$ )<sup>22,24</sup> and to the

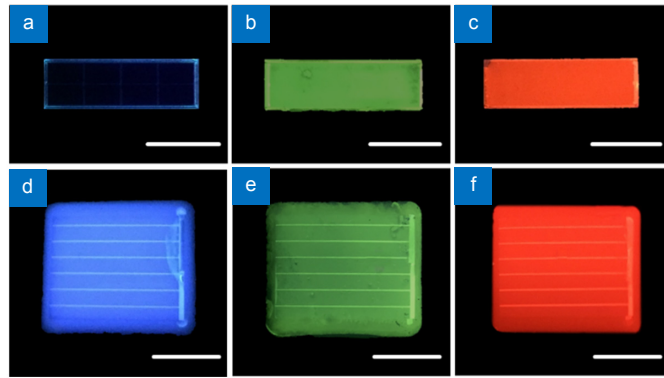


**Fig. 1 |** Photographs of the (a, d) bare PV devices and of the coated (b, c) PV-1 and (e, f) PV-2 with the (b, e) dU6-Tb and (c, f) tU5-Eu LDS layers, under UV radiation at 365 nm. Scale bars:  $10^{-2}$  m.

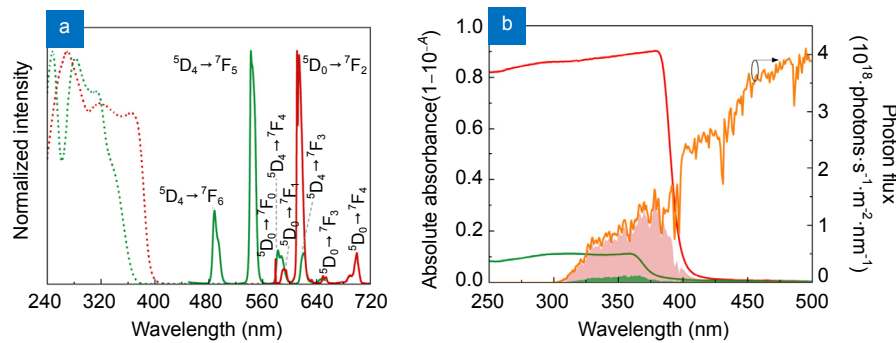


**Fig. 2 |** (a) Excitation spectra (dashed lines) monitored at 543 nm and 615 nm for dU6-Tb (green line) and tU5-Eu (red line), and emission spectra (solid lines) excited at 315 nm for dU6-Tb (green line), and 365 nm for tU5-Eu (red line); (b) Absorption spectra of dU6-Tb and tU5-Eu and AM1.5G photon flux (right y axis). The shadowed areas represent the overlap integral, Eq. (3), with the same colour code as the excitation and emission spectra.

d-U(600) host ( $\sim 350$  nm)<sup>31</sup>. For tU5-Eu the spectrum shows three main components peaking at 270, 320 and 365 nm, mainly ascribed to the hybrid host<sup>30</sup> and to the tta triplet states<sup>26,32</sup>, respectively. The 320 and 365 nm components resemble those already observed for isolated  $\text{Eu}(\text{tta})_3 \cdot 2\text{H}_2\text{O}$ <sup>33</sup> and for organic-inorganic hybrids incorporating  $\text{Eu}(\text{tta})_3 \cdot 2\text{H}_2\text{O}$  and  $\text{Eu}(\text{tta})_3(\text{phen})$  ( $\text{phen} = 1,10$ -phenanthroline), being ascribed to the  $\pi-\pi^*$  electronic transition of the organic ligands<sup>34</sup>. Apart from changes in the relative intensity, the UV-visible absorption spectra, Fig. 2(b), reveal the same components detected in excitation spectra.

Featuring PV related applications, and in order to maximize the performance of LSCs, it is relevant to quantify the light harvesting ability<sup>35</sup>, which can be done by estimating the overlap integral between the materials absorbance and the sunlight available for PV conversion. The overlap integral, presented in Fig. 2(b), is given by<sup>36</sup>:

$$O = \int_{\lambda_1}^{\lambda_2} \Phi_{\text{AM1.5G}}(\lambda) \times (1 - 10^{-A(\lambda)}) d\lambda, \quad (3)$$

where  $\lambda_1$  and  $\lambda_2$  are the limits of the spectral overlap between the absorption spectrum of dU6-Tb and tU5-Eu and the AM1.5G spectrum,  $\Phi_{\text{AM1.5G}}$  is the AM1.5G photon flux and  $A$  is the absorbance of tU5-Eu and dU6-Tb. A value of  $8.8 \times 10^{18}$  photons $\cdot$ s $^{-1}$  $\cdot$ m $^{-2}$  was found for dU6-Tb and for tU5-Eu, the value was  $6.8 \times 10^{19}$  photons $\cdot$ s $^{-1}$  $\cdot$ m $^{-2}$ .

These values indicate that these LDS coatings have, respectively, the potential to absorb  $\sim 0.2\%$  and  $\sim 1.6\%$  of the solar photon flux on the Earth surface ( $4.3 \times 10^{21}$  photons $\cdot$ s $^{-1}$  $\cdot$ m $^{-2}$  $\cdot$ nm $^{-1}$ )<sup>5</sup>.

The emission properties of the LDS coatings were further quantified through the measurement of the absolute  $\Phi$  values, with maxima for dU6-Tb of  $0.55 \pm 0.06$  (350 nm) and  $0.56 \pm 0.06$  (320 nm) for tU5-Eu. The values found for the  $\text{Eu}^{3+}$ -based organic-inorganic hybrid materials are of the same order of magnitude of the ones previously reported<sup>27-29</sup>, being remarkable the value here reported for dU6-Tb, higher than the 0.25 and 0.32 values found for  $\text{Ln}^{3+}$  coordination polymers doped with  $\text{Tb}^{3+}$ <sup>37</sup> and that of bipyridine-based bridged silsesquioxanes and d-U(600) organic-inorganic hybrids containing  $\text{Tb}^{3+}$  with maximum absolute  $\Phi$  values of  $0.12 \pm 0.01$ <sup>38</sup> and  $0.11 \pm 0.01$ <sup>39</sup>, respectively.

The effect of the coating on the surface reflection of the PV cells may be quantified by the Haze factor. The Haze factor refers to the degree of incident light scattered forward towards the absorber layer. It can be described by the ratio between the diffuse reflectance ( $R_{\text{diffuse}}$ ) and total reflectance ( $R_{\text{total}}$ )<sup>40,41</sup>:

$$\text{Haze} = \frac{R_{\text{diffuse}}}{R_{\text{total}}}, \quad (4)$$

Larger Haze values correspond to increased scattering and hence an increased optical path length, which is of critical importance to improve light absorption<sup>40,41</sup>. Thus, considering this aspect, the LDS coatings presented here are good candidates to be used in PV cells. As evidenced in Fig. 3, the total reflectance of the bare PV devices is always higher than the diffuse one. After the deposition, the diffuse and total reflectance curves come closer, meaning that the specular component of the reflectance is decreased. Therefore, it is expected an increase in the Haze factor for all the coatings considering the 300 to 800 nm spectral range.

The active role of the mentioned LDS coatings in enhancing the PV device performance was inferred from the EQE curves of PV-1 and PV-2 devices with and without the presence of the LDS coatings. An enhancement of the PV cell performance in the UV spectral region was verified for all the PV devices with the LDS coatings, Fig. 4.

As shown in Fig. 4, an increase in the EQE is noticeable

in the UV/blue region between 300 and 360 nm, which is the spectral range where Si PV cells have lower performance and, also, corresponds to the maximum absorption region of the produced LDS coatings. We note that PV cells coated with a non-doped hybrid layer yield no changes in the PV performance (Fig. S5 in ESI) reinforcing that the main contribution for such PV cells enhancement in the presence of the LDS coatings arises from the UV-down-shifted converted photons. In particular, a maximum absolute increase of ~27% was found for the dU6-Tb LDS coating (for 320 nm incident radiation) on PV-2 (Table 1), resulting from a relative increase of ~4 in the  $I_{sc}$  in the same region (Fig. S6 in ESI). The V-P curves of all solar devices (Fig. 5) were measured under AM1.5G illumination, and the relative increase of the electrical power generated by the PV cell with the LDS coating was inferred through:

$$\Delta P = \frac{\int_0^{V_{oc}} P_{coated}(dV) - \int_0^{V_{oc}} P_{bare}(dV)}{\int_0^{V_{oc}} P_{coated}(dV)} \times 100 \quad (5)$$

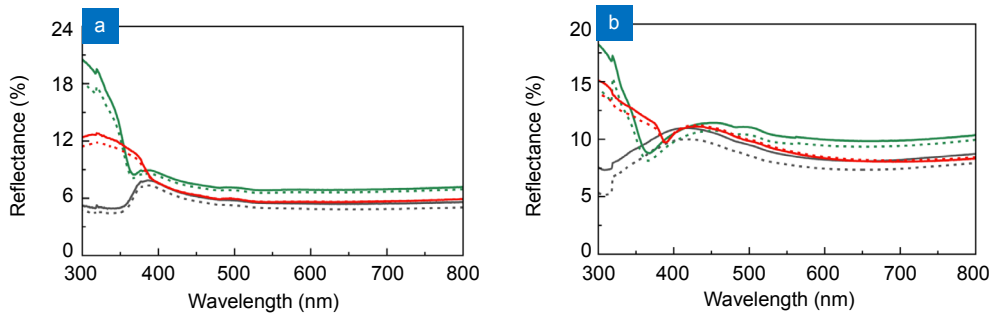


Fig. 3 | Total (solid lines) and diffuse (dashed lines) reflectance of (a) PV-1 and (b) PV-2 with dU6-Tb (green lines) and tU5-Eu (red lines) coatings compared with the average reflectance curve measured for distinct bare PV devices (black lines).

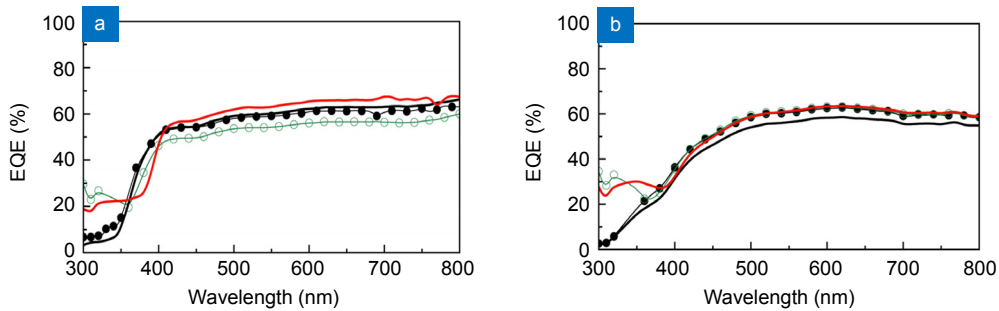


Fig. 4 | EQE curves of (a) PV-1 and (b) PV-2 with dU6-Tb (green dotted lines) and tU5-Eu (red solid lines) coatings compared with the correspondent bare PV devices (black lines).

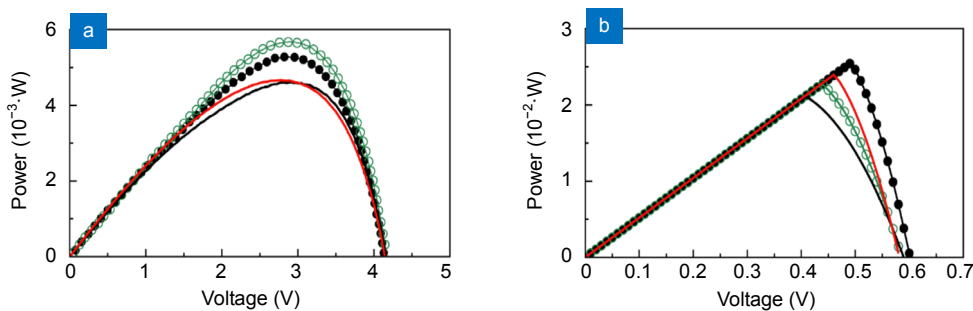


Fig. 5 | V-P curves of (a) PV-1 and (b) PV-2 with dU6-Tb (green dotted lines) and tU5-Eu (red solid lines) coatings compared with the correspondent bare PV devices (black lines).

in which  $V_{oc}$  is the open-circuit voltage of the PV device,  $P_{coated}$  is the power generated by the PV device with the LDS coating and  $P_{bare}$  is the power generated by the bare PV device. The maximum power relative increase value was 9%, found for PV-2 with tU5-Eu LDS coating, Fig. 5(b), comparing with the values of 7% and 2% found for PV-1 with the dU6-Tb and tU5-Eu LDS coatings, respectively. For the PV-2 device with the dU6-Tb LDS coating, a decrease of 11% was verified, probably due to the fact of the dU6-Tb emission being less resonant with Si absorption, when compared to the tU5-Eu case. The fact that this is not happening for the PV-1 cases, may be caused by the differences in the surface reflectance of the bare PV cell, which is higher for the PV-2 cases.

These results are very promising and among the highest values reported for  $\text{Ln}^{3+}$ -based LDS coatings<sup>19,42</sup> mentioned in Table 1, except for the case of a LDS layer based on  $\text{Eu}(\text{tta})_3 \cdot 2\text{H}_2\text{O}$  complex with 4,5-bis(pinene)-2,2'-bipyridine ligand dispersed in polyvinyl acetate (PVA), which presented an absolute EQE increase of ~50%<sup>13</sup>.

**Table 1 | Reported absolute EQE increase in the UV spectral region for  $\text{Ln}^{3+}$ -based LDS coatings.**

Optically active layer	PV device	EQE increase
dU6-Tb [this work]	PV-1	19%
tU5-Eu [this work]		17%
dU6-Tb [this work]	PV-2	27%
tU5-Eu [this work]		23%
Eu-doped phosphor/Ag nanoparticles/ $\text{SiO}_2$ <sup>8</sup>	c-Si	12%
Eu-doped phosphor/ $\text{SiO}_2$ <sup>7</sup>		8%
Eu-doped phosphor/ $\text{SiO}_2$ <sup>6</sup>		7%
Eu-doped phosphor/ $\text{SiO}_2$ <sup>12</sup>		10%
$[\text{Eu}(\text{tta})_3(\text{tppo})_2]/\text{EVA}$ <sup>19</sup>		19%
$\text{Eu}(\text{tta})_3(\text{phen})/\text{EVA}$ <sup>19</sup>		17%
$[\text{EuL}_3]/\text{EVA}$ <sup>19</sup>		15%
$[\text{TbL}_3]/\text{EVA}$ <sup>19</sup>		15%
$[\text{Eu}(\text{tta})_3(\text{bppy})]/\text{PVA}$ <sup>13</sup>		50%
$[\text{Eu}(\text{tfc})_3:\text{EABP}] 1:1/\text{EVA}$ <sup>16</sup>		5%
$[\text{Eu}(\text{tfc})_3/\text{Eu}(\text{dbm})_3\text{phen}]/\text{PVA}$ <sup>15</sup>		5%
$\text{Ba}_2\text{SiO}_4:\text{Eu}^{2+}$ <sup>43</sup>		3%
$\text{SiO}_2/\text{Ba}_2\text{SiO}_4:\text{Eu}^{2+}$ <sup>44</sup>		3%
$\text{LaVO}_4/\text{Dy}^{3+}$ <sup>45</sup>		2%
$\text{EuD}_4\text{TEA}$ <sup>42</sup>		DSSC

EVA=ethylene-vinyl acetate; PVA=polyvinyl acetate; tppo=triphenylphosphine oxide; phen=1,10-phenanthroline;  $\text{L}_3$ =triazole-pyridine-bistetrazolate; bppy=4,5-bis(pinene)-2,2'-bipyridine;  $\text{Eu}(\text{tfc})_3$ =tris[3-(trifluoromethylhydroxymethyl)-d-camphor]europium(III); EABP=4,4'-bis(diethylamino)benzophenone; dbm=dibenzoylmethane;  $\text{EuD}_4\text{TEA}$ =europium tetrakis dibenzoylmethide triethylammonium; DSSC=dye-sensitized solar cell.

To illustrate the concept of enhancing PV cells performance using LDS coatings, the PV-2 devices were coupled to a wheeled structure composing a small solar vehicle, and a race between solar vehicles with bare and coated PV-2 devices was performed in horizontal plane (Fig. 6 and Fig. S7 in ESI). For this test, the tU5-Eu LDS coating was chosen due to the presented relative gain in the delivered power compared with the bare cell. The solar vehicle using the tU5-Eu LDS coating was the winner, with a relative increase in the velocity of ~9% compared with the device with the bare PV-2, which is similar to the power relative increase value above mentioned. Moreover, if we consider the EQE curve of this device and estimate the relative EQE increase over the AM1.5G spectra (in the 300 to 800 nm spectral range), through:

$$\Delta EQE_{\text{AM1.5G}} = 100 \times \left[ 1 - \frac{\int_{300}^{800} EQE_{\text{bare}}(\lambda) \times I_{\text{AM1.5G}}(\lambda)}{\int_{300}^{800} EQE_{\text{coated}}(\lambda) \times \Phi_{\text{AM1.5G}}(\lambda)} \right], \quad (6)$$

in which  $EQE_{\text{coated}}$  is the EQE of the PV device with the LDS coating and  $EQE_{\text{bare}}$  is the EQE of the bare PV device, we found a value of ~9% (Table S1 in ESI) in good agreement with the velocity and relative power increase, suggesting that the verified increase in the velocity of the solar vehicle with the coated PV cell is due to an efficient UV to visible photon conversion performed by the tU5-Eu LDS coating.

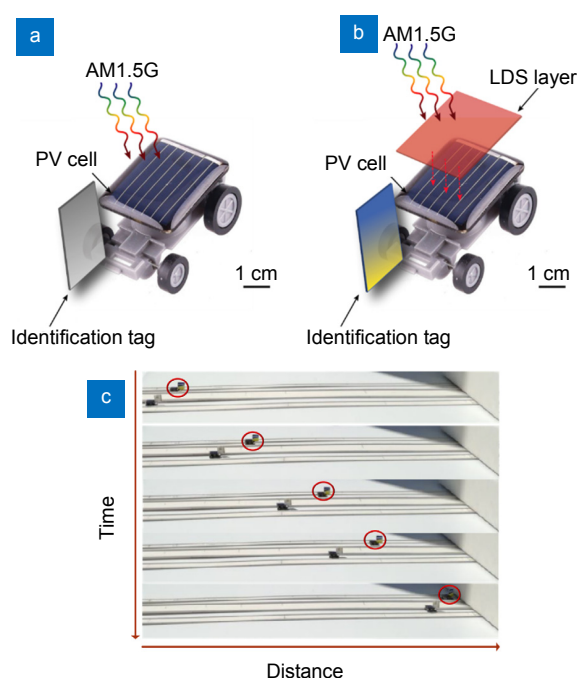


**Fig. 6 | Scheme of the solar vehicle with (a) bare PV-2 and (b) PV-2 with the LDS coating and (c) photographs of the solar vehicles race. The solar vehicle with the coated PV cell is indicated by the red circle.**

## Conclusions

In this work, luminescent downshifting (LDS) coatings

based on  $\text{Eu}^{3+}$  and  $\text{Tb}^{3+}$ -doped organic-inorganic hybrid materials are reported. These materials are able to absorb the UV component of the solar irradiance on Earth (absorption at 300–400 nm) and present emission in the visible spectral regions. The performance of the LDS coating coupled to a c-Si PV cell was evaluated and a maximum absolute increase in the PV cell external quantum efficiency of ~27% was observed between 300 and 400 nm. The concept and applicability of these LDS coatings were visually proved by a race between small solar vehicles with bare and coated PV cells, in which the solar car with the  $\text{Eu}^{3+}$ -based LDS coating on the PV cell presented a relative increase in the velocity of ~9%, comparing with the one with the bare PV cell. These LDS layers proved its ability to be used in c-Si solar cells which are still the most common technology in use but they may also be used in perovskite-based technologies which, although not commercially available, are worth noting. In general, both these types of PV cells present low spectral response in the UV spectral region and thus, the UV LDS layers presented here may be suitable and advantageous.

## References

- Nann S, Riordan C. Solar Spectral irradiance under clear and cloudy skies: measurements and a semiempirical model. *J Appl Meteorol* **30**, 447–462 (1991).
- Shimokawa R, Miyake Y, Nakanishi Y, Kuwano Y, Hamakawa Y. Effect of atmospheric parameters on solar cell performance under global irradiance. *Sol Cells* **19**, 59–72 (1986).
- Alboteanu I, Bulucea C, Degeratu S. Estimating solar irradiation absorbed by photovoltaic panels with low concentration located in Craiova, Romania. *Sustainability* **7**, 2644–2661 (2015).
- Huang X, Han S, Huang W, Liu X. Enhancing solar cell efficiency: the search for luminescent materials as spectral converters. *Chem Soc Rev* **42**, 173–201 (2013).
- Bünzli J-C G, Chauvin A-S. *Handbook on the Physics and Chemistry of Rare-Earths* (Elsevier B. V., Amsterdam), 169–281 (2014).
- Ho W-J, Deng Y-J, Liu J-J, Feng S-K, Lin J-C *et al.* Photovoltaic performance characterization of textured silicon solar cells using luminescent down-shifting Eu-doped phosphor particles of various dimensions. *Materials* **10**, 21 (2017).
- Ho W-J, You B-J, Liu J-J, Bai W-B, Syu H-J *et al.* Photovoltaic performance enhancement of silicon solar cells based on combined ratios of three species of Europium-doped phosphors. *Materials* **11**, 845 (2018).
- Ho W-J, Feng S-K, Liu J-J, Yang Y-C, Ho C-H. Improving photovoltaic performance of silicon solar cells using a combination of plasmonic and luminescent downshifting effects. *Appl Surf Sci* **439**, 868–875 (2018).
- Klampfittis E, Ross D, McIntosh K R, Richards B S. Enhancing the performance of solar cells via luminescent down-shifting of the incident spectrum: A review. *Sol Energy Mater Sol Cells* **93**, 1182–1194 (2009).
- Klampfittis E, Richards B S. Improvement in multi-crystalline silicon solar cell efficiency via addition of luminescent material to EVA encapsulation layer. *Prog Photovoltaics Res Appl* **19**, 345–351 (2011).
- Kataoka H, Omagari S, Nakanishi T, Hasegawa Y. EVA thin film with thermo- and moisture-stable luminescent copolymer beads composed of Eu(III) complexes for improvement of energy conversion efficiency on silicon solar cell. *Opt Mater* **42**, 411–416 (2015).
- Ho W-J, Shen Y-T, Liu J-J, You B-J, Ho C-H *et al.* Enhancing photovoltaic performance using broadband luminescent down-shifting by combining multiple species of Eu-doped silicate phosphors. *Nanomaterials* **7**, 340 (2017).
- Liu J, Wang K, Zheng W, Huang W, Li C H *et al.* Improving spectral response of monocrystalline silicon photovoltaic modules using high efficient luminescent down-shifting  $\text{Eu}^{3+}$  complexes. *Prog Photovoltaics* **21**, 668–675 (2013).
- Monzón-Hierro T, Sanchiz J, González-Pérez S, González-Díaz B, Holinski S *et al.* A new cost-effective polymeric film containing an Eu(III) complex acting as UV protector and down-converter for Si-based solar cells and modules. *Sol Energy Mater Sol Cells* **136**, 187–192 (2015).
- Le Donne A, Acciarri M, Narducci D, Marchionna S, Binetti S. Encapsulating  $\text{Eu}^{3+}$  complex doped layers to improve Si-based solar cell efficiency. *Prog Photovoltaics* **17**, 519–525 (2011).
- Le Donne A, Dilda M, Crippa M, Acciarri M, Binetti S. Rare earth organic complexes as down-shifters to improve Si-based solar cell efficiency. *Opt Mater* **33**, 1012–1014 (2011).
- González-Pérez S, Sanchiz J, González-Díaz B, Holinski S, Borchert D *et al.* Luminescent polymeric film containing an Eu(III) complex acting as UV protector and down-converter for Si-based solar cells and modules. *Surf Coatings Technol* **271**, 106–111 (2015).
- Kin E, Fukuda T, Yamauchi S, Honda Z, Ohara H *et al.* Thermal stability of europium(III) chelate encapsulated by sol-gel glass. *J Alloys Compd* **480**, 908–911 (2009).
- Fix T, Nonat A, Imbert D, Di Pietro S, Mazzanti M *et al.* Enhancement of silicon solar cells by downshifting with Eu and Tb coordination complexes. *Prog Photovoltaics Res Appl* **24**, 1251–1260 (2016).
- Yang Y, Zhang S. Study of lanthanide complexes with salicylic acid by photoacoustic and fluorescence spectroscopy. *Spectrochim Acta Part A Mol Biomol Spectrosc* **60**, 2065–2069 (2004).
- Wu R, Zhao H, Su Q. Photoacoustic and fluorescence studies of silica gels doped with rare earth salicylic acid complexes. *J Non-Cryst Solids* **278**, 223–227 (2000).
- Misra V, Mishra H. Photoinduced proton transfer coupled with energy transfer: Mechanism of sensitized luminescence of terbium ion by salicylic acid doped in polymer. *J Chem Phys* **128**, 244701 (2008).
- Li S W, Song H W, Li W L, Ren X G, Lu S Z *et al.* Improved photoluminescence properties of ternary terbium complexes in mesoporous molecule sieves. *J Phys Chem B* **110**, 23164–23169 (2006).
- Fan X, Wang Z, Wang M. In situ synthesis kinetics of salicylic acid terbium complexes in sol-gel derived host materials. *J Sol-Gel Sci Technol* **30**, 95–99 (2004).
- de Zea Bermudez V, Carlos L D, Alcácer L. Sol-gel derived urea cross-linked organically modified silicates. 1. Room temperature mid-infrared spectra. *Chem Mater* **11**, 569–580 (1999).
- Molina C, Dahmouche K, Messaddeq Y, Ribeiro S J L, Silva M A P *et al.* Enhanced emission from Eu(III)  $\beta$ -diketone complex combined with ether-type oxygen atoms of di-ureasil organic-inorganic hybrids. *J Lumin* **104**, 93–101 (2003).
- Correia S F H, Lima P P, Pecoraro E, Ribeiro S J L, André P S

- et al.* Scale up the collection area of luminescent solar concentrators towards metre-length flexible waveguiding photovoltaics. *Prog Photovoltaics Res Appl* **24**, 1178–1193 (2016).
28. Correia S F H, Frias A R, Fu L, Rondão R, Pecoraro E *et al.* Large-area tunable visible-to-near-infrared luminescent solar concentrators. *Adv Sustain Syst* **2**, 1800002 (2018).
  29. Correia S F H, Lima P P, André P S, Ferreira R A S, Carlos L D. High-efficiency luminescent solar concentrators for flexible waveguiding photovoltaics. *Sol Energy Mater Sol Cells* **138**, 51–57 (2015).
  30. Freitas V T, Lima P P, Ferreira R A S, Pecoraro E, Fernandes M *et al.* Luminescent urea cross-linked tripodal siloxane-based hybrids. *J Sol-Gel Sci Technol* **65**, 83–92 (2013).
  31. Carlos L D, de Zea Bermudez V, Ferreira R A S, Marques L, Assunção M. Sol-gel derived urea cross-linked organically modified silicates. 2. Blue-light emission. *Chem Mater* **11**, 581–588 (1999).
  32. Nolasco M M, Vaz P M, Freitas V T, Lima P P, André P S *et al.* Engineering highly efficient Eu(III)-based tri-ureasil hybrids toward luminescent solar concentrators. *J Mater Chem A* **1**, 7339–7350 (2013).
  33. Kai J A, Felinto M C F C, Nunes L A O, Malta O L, Brito H F. Intermolecular energy transfer and photostability of luminescence-tunable multicolour PMMA films doped with lanthanide-beta-diketonate complexes. *J Mater Chem* **21**, 3796–3802 (2011).
  34. Fernandes M, de Zea Bermudez V, Ferreira R A S, Carlos L D, Charas A *et al.* Highly photostable luminescent poly (E-caprolactone) siloxane biohybrids doped with europium complexes. *Chem Mater* **19**, 3892–3901 (2007).
  35. Reisfeld R, Shamrakov D, Jorgensen C. Photostable solar concentrators based on fluorescent glass-films. *Sol Energy Mater Sol Cells* **33**, 417–427 (1994).
  36. Rondão R, Frias A R, Correia S F H, Fu L, de Zea Bermudez V *et al.* High-performance near-infrared luminescent solar concentrators. *ACS Appl Mater Interfaces* **9**, 12540–12546 (2017).
  37. Gai Y, Jiang F, Chen L, Wu M, Su K *et al.* Europium and terbium coordination polymers assembled from hexacarboxylate ligands: structures and luminescent properties. *Cryst Growth Des* **14**, 1010–1017 (2014).
  38. Graffion J, Cojocariu A M, Cattoeen X, Ferreira R A S, Fernandes V R *et al.* Luminescent coatings from bipyridine-based bridged silsesquioxanes containing Eu<sup>3+</sup> and Tb<sup>3+</sup> salts. *J Mater Chem* **22**, 13279–13285 (2012).
  39. Lima P P, Ferreira R A S, Alves Junior S, Malta O L, Carlos L D. Terbium(III)-containing organic-inorganic hybrids synthesized through hydrochloric acid catalysis. *J Photochem Photobiol A-Chemistry* **201**, 214–221 (2009).
  40. Mahadik D B, Lakshmi R V, Barshilia H C. High performance single layer nano-porous antireflection coatings on glass by sol-gel process for solar energy applications. *Sol Energy Mater Sol Cells* **140**, 61–68 (2015).
  41. Preston C, Xu Y L, Han X G, Munday J N, Hu L B. Optical haze of transparent and conductive silver nanowire films. *Nano Res* **6**, 461–468 (2013).
  42. Griffini G, Bella F, Nisic F, Dragonetti C, Roberto D *et al.* Multi-functional luminescent down-shifting fluoropolymer coatings: a straightforward strategy to improve the UV-light harvesting ability and long-term outdoor stability of organic dye-sensitized solar cells. *Adv Energy Mater* **5**, 1401312 (2015).
  43. Bin Hung W, Chen J Y, Sung K W, Chen T M. Enhanced conversion efficiency of crystalline Si solar cells via luminescent down-shifting using Ba<sub>2</sub>SiO<sub>4</sub>:Eu<sup>2+</sup> phosphor. *J Ceram Process Res* **15**, 157–161 (2014).
  44. Chen J-Y, Huang C K, Hung W B, Sun K W, Chen T M. Efficiency improvement of Si solar cells using metal-enhanced nanophosphor fluorescence. *Sol Energy Mater Sol Cells* **120**, 168–174 (2014).
  45. Liu J F, Yao Q H, Li Y D. Effects of downconversion luminescent film in dye-sensitized solar cells. *Appl Phys Lett* **88**, 173119 (2006).

### Acknowledgements

This work was developed within the scope of the project CICECO-Aveiro Institute of Materials, (UID/CTM/50011/2019), Instituto de Telecomunicações (UID/EEA/50008/2019), Solar-Flex (CENTRO-01-0145-FEDER-030186), and SusPhotoSolutions (CENTRO-01-0145-FEDER-000005) financed by national funds through the FCT/MEC and when appropriate co-financed by FEDER under the PT2020 Partnership through European Regional Development Fund (ERDF) in the frame of Operational Competitiveness and Internationalization Programme (POCI). L. S. F. and A. R. N. B. thank WINLEDs (POCI-01-0145-FEDER-030351) and NanoHeatControl (POCI-01-0145-FEDER-031469), respectively. Joaquim Almeida from Escola Secundária de Oliveira do Bairro, Portugal is acknowledged for providing the photo finish images.

### Author contributions

R. A. S. F., P. S. A., L. D. C. and S. F. H. C. designed the experiments, interpreted the data and co-wrote the paper. L. S. F., S. F. H. C. and A. R. N. B. carried out the synthesis, characterization, optical measurements and data analysis.

### Competing interests

The authors declare no competing financial interests.

### Supplementary information

Supplementary information for this paper is available at <https://doi.org/10.29026/oea.2019.190006>